Towards functional organ preservation in head and neck cancer

Doornaert, P.

2016

document version
Publisher's PDF, also known as Version of record

Chapter 7

Use of diffusion-weighted magnetic resonance imaging (DW-MRI) to investigate the effect of chemo-radiotherapy on the salivary glands

Patricia Doornaert[a], Max Dahele[a], Redina Ljumanovic[b], Remco de Bree[c], Ben J Slotman[a], Jonas A Castelijns[b]

[a]*Department of Radiation Oncology, VU University Medical Center, Amsterdam, the Netherlands*

[b] *Department of Radiology and Nuclear Medicine, VU University Medical Center, Amsterdam, the Netherlands*

[c] *Department of Otolaryngology and Head and Neck Surgery, VU University Medical Center, Amsterdam, the Netherlands*

Acta Oncol. 2015;54:1068-71

Introduction

Chemo-radiotherapy (CRT) is the standard treatment for locally advanced head and neck cancer (HNC), offering comparable survival to surgery with the benefit of organ preservation. However one of the most troublesome side-effects is parotid (PG) and submandibular gland (SMG) toxicity leading to loss of gland function and hypo-salivation. The mechanism of salivary gland toxicity is incompletely understood and interventions for preventing or reversing hypo-salivation are currently limited [1]. The use of intensity-modulated radiotherapy (IMRT) to reduce salivary gland dose is now routine, but it is only partially effective [2,3]. Non-invasive imaging might help to better understand the response of the glands to CRT and identify salivary gland toxicity. This could in turn help to develop therapeutic strategies. A previous report suggested that diffusion-weighted magnetic resonance imaging (DW-MRI) before and after treatment might be a promising tool for investigating changes due to radiotherapy [4]. Our goal was to image the effect of CRT on salivary glands using DW-MRI performed before, during and after CRT. Although DW-MRI in HNC is often performed with echo planar imaging (EPI) sequences, this technique is particularly prone to geometric distortions due to susceptibility artefacts. To overcome these possible disadvantages, we also used a non-EPI technique, (half-fourier acquisition single-shot turbo spin-echo, HASTE) [5]. Taking into account work that suggests heterogenous effects of radiation within glands, and different responses in PG and SMG, we analyzed sub-regions within individual glands and evaluated the parotid and submandibular glands separately [6-8]. We also looked for correlations between DW-MRI changes and planned radiation dose. In comparison with previous literature, the use of 2 different DW-MRI sequences, analysis of sub-regions in the glands and availability of imaging during, as well as before and after CRT, are strengths of this study.

Materials and methods

Patients

The present report describes an analysis of imaging data from a prospective institutional study investigating DW-MRI and tumor control [9]. All patients had combined modality treatment for locally advanced HNC: 7 patients had an oropharynx and 1 patient a hypopharynx carcinoma; 4 had cisplatin-based CRT, 2 had cetuximab-based CRT and 2 had induction-chemotherapy with cetuximab and TPF (docetaxel, cisplatin, 5-fluorouracil) followed by cisplatin-based CRT. MRI scans made on the same scanner (1.5 Tesla Sonata, Siemens, Erlangen, Germany) were available for 8 patients before and during CRT, and 5/8 patients after CRT (3 patients had post-treatment scans on another machine and were not analyzed).

Radiotherapy

All patients had a contrast enhanced planning computed tomography (CT) scan (2.5mm slice thickness) in an immobilization mask. Dose prescription was either 54.25Gray (Gy) (1.55Gy/fraction; n=2) or 57.75Gy (1.65Gy/fraction; n=6) to the elective regions and 70Gy (2Gy/fraction) to the primary tumor delivered as a simultaneous integrated boost. Treatment planning was performed using the Eclipse™ treatment planning system (Varian Medical Systems, Palo Alto, USA).

MRI examinations

The baseline MRI scans (DW-MRI_1) were made before the start of chemotherapy and radiotherapy (range 0-24 days before RT, 102-114 days before RT in patients receiving induction CT). A second DW-MRI (DW-MRI_2) was performed after the delivery of 20 (n=7) or 22 (n=1) Gray (Gy) to the tumor, and a third MRI examination (DW-MRI_3), available in 5 patients, was made 2-3 months (70-91 days) after completion of therapy. For all examinations, a head coil combined with a phased array spine and neck coil was used and axial MR images were acquired (22 slices with 4mm slice thickness), centred on the primary tumor and enlarged nodes. EPI parameters were: TR/TE=5000/105ms, in-plane pixel size=2x2mm, and b-values=0, 500 and 1000s/mm^2 (3 averages). Parameters for HASTE were: TR/TE=900/110ms, in-plane pixel size=1.1x1.1mm, and b-values=0s/mm2 (3 averages) and 1000s/mm^2 (12 averages). The ADC maps were calculated using the software of the MRI machine (units of $10^{-5}mm^2/s$) .

Regions of interest (ROIs) within salivary glands

Ten 7mm diameter spherical ROIs were defined for each patient on the planning CT scan: 3 in each PG (upper part, lower part and deep lobe) and 2 in each SMG (anterior and posterior). For each patient a diagram of the ROI location was generated. Using this diagram, a corresponding ROI was drawn on each of the DW-MRIs and the ADC value was recorded.

Analysis

In this small study, only simple descriptive statistics were used.

Results

The pooled data for all ROIs is summarized in Table 1. In the 5 patients with DW-MRI data after treatment, the mean dose to the entire ipsilateral (IL) and contralateral (CL) PG was 43.9Gy (± 6Gy standard deviation, SD) and 31.4Gy (± 6.6Gy SD), respectively. The SMGs received a mean dose of 59.4Gy-73.2Gy. The mean dose to the upper PG was the lowest of all ROIs: 6.0Gy (IL) and 2.9Gy (CL) after approximately 2 weeks of CRT, and 21.1Gy (IL) and 11.8Gy (CL) after the completion of treatment. In all time periods, EPI and HASTE ADC values were lower for the PG than the SMG. When comparing the PG ROIs, in all time periods, including prior to treatment, there was a difference in ADC results for both EPI and HASTE imaging, with the lower and deep ROIs having higher ADC values than the upper ROIs.

Table 1: Radiation (RT) doses and ADC values for EPI and HASTE DW-MRI before, during and after treatment for different regions of interest (ROI) in the ipsilateral (IL) and contralateral (CL) parotid (PG) and submandibular glands (SMG). Values presented as mean (standard deviation)

		Baseline (n=8)		**During (n=8)**			**After (n=5)**		
	ROI	**HASTE ADC[a]**	**EPI ADC**	**HASTE ADC**	**EPI ADC**	**RT Dose[b]**	**HASTE ADC**	**EPI ADC**	**RT dose**
IL PG	upper	67 (28)	76 (20)	60 (16)	76 (31)	6,0 (3,3)	97	111 (13)	21.1 (7.6)
	lower	76 (22)	96 (16)	82 (15)	115 (23)	14.7 (4.0)	100 (26)	136 (10)	53.8 (16.1)
	deep	78 (22)	89 (11)	73 (12)	100 (35)	18.7 (1.8)	106 (25)	125 (16)	67.5 (5.9)
CL PG	upper	68 (22)	77 (21)	61 (24)	66 (30)	2.9 (0.9)	85 (31)	106 (25)	11.8 (2.0)
	lower	73 (19)	87 (14)	73 (20)	112 (23)	10.1 (4.9)	100 (31)	125 (27)	38.4 (19.8)
	deep	76 (25)	88 (15)	77 (19)	99 (31)	13.9 (5.8)	105 (37)	117 (26)	54.2 (20.6)
IL SMG	anterior	82 (26)	110 (13)	99 (15)	135 (14)	18.4 (3.2)	125 (26)	152 (13)	66.9 (8.4)
	posterior	80 (24)	107 (13)	100 (18)	133 (11)	20.4 (1.3)	125 (25)	151 (11)	72.8 (1.0)
CL SMG	anterior	83 (29)	108 (15)	97 (20)	129 (12)	14.7 (7.0)	120 (24)	147 (10)	62.7 (5.1)
	posterior	81 (27)	109 (11)	99 (21)	132 (11)	18.0 (2.9)	118 (17)	144 (11)	67.5 (5.9)

[a]ADC values in units of $x10^{-5}mm^2/s$. [b]RT dose in Grays

During treatment

When all PG and SMG ROIs were taken together, both EPI and HASTE ADC values were higher after approximately 2 weeks of treatment that at baseline (mean 94 before treatment versus 111 during treatment for EPI, and 76 before treatment versus 83 during treatment for HASTE). When considering PG and SMG ROIs separately, the rise in ADC values for both PG and SMG was most noticeable using EPI DW-MRI (PG: mean 84 before treatment versus 95 during treatment and for SMG: mean 109 before treatment versus 132 during treatment). Considering all ROIs together, the correlation between the dose received early in treatment and the change (Δ) in ADC (Spearman's rank coefficient) was r=0.23 for EPI and r=0.38 for HASTE.

After treatment

For the combined PG and SMG ROIs there was an increase in EPI and HASTE ADC values after treatment compared with baseline (mean 94 before treatment versus 131 after treatment with EPI, and 75 before treatment versus 108 after treatment with HASTE; Table 1). Taking all ROIs together, the correlation between the total dose received by the ROI and ΔADC for the HASTE technique was r=0.33, and r=0.11 for the EPI technique.

Figure 1a: Change in HASTE DW-MRI ADC values 3 months after therapy versus radiotherapy dose. Spearman's rank coefficient for all ROIs together 0.33

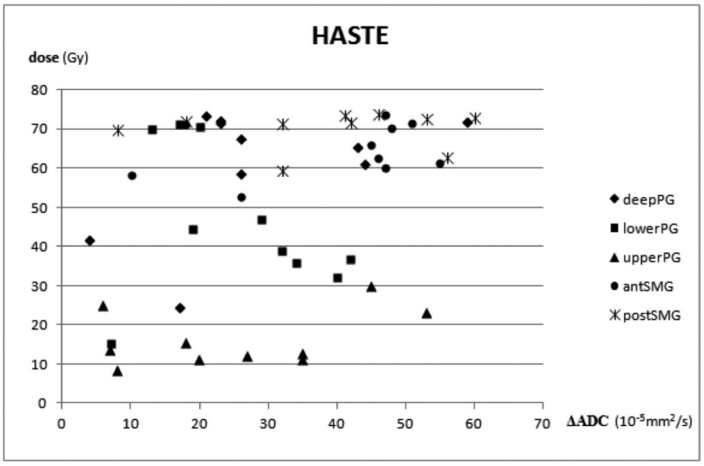

Figure 1b: Change in EPI DW-MRI ADC values 3 months after therapy versus radiotherapy dose. Spearman's rank coefficient for all ROIs together 0.11

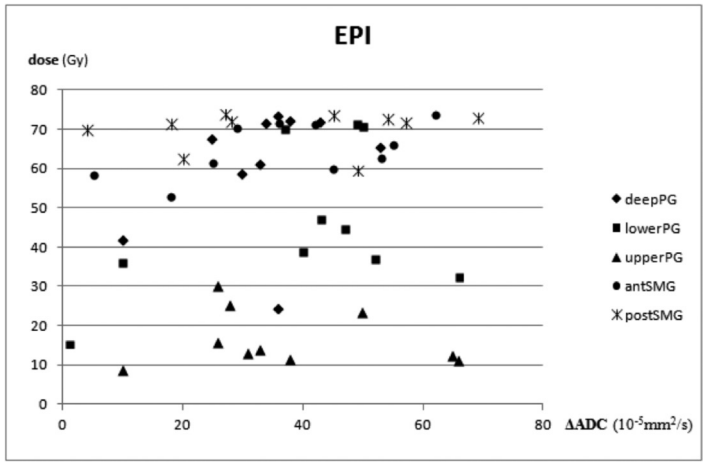

Discussion

Two different DW-MRI techniques were used to explore changes in the salivary glands approximately 2 weeks into and 3 months after CRT for head and neck cancer. Both MRI techniques showed a rise in PG and SMG ADC during and after CRT. ADC values with both EPI and HASTE were lower in the PG than the SMG and with both techniques there appeared to regional differences within the PG and SMG. HASTE showed a better correlation between dose and ΔADC between baseline and during/after CRT.

We observed an increase in all PG and SMG ADC values after CRT and found no difference between IL and CL ADC values. This is in contrast to Dirix et al [8], who found a significant difference in whole-gland ADC values before and 6 months after RT in the IL, but not in the CL PG. This could be due to the fact that the dose difference between the IL and CL PG was much larger in the series from Dirix (33.9Gy versus 12.5Gy) and our post-treatment imaging may be too soon after treatment [7].

Several limitations of this study should be mentioned, including the following: (1) The most apparent is the small sample size, which prevented more detailed statistical analysis; (2) There were differences in treatment schedule and chemotherapy/biological agents; (3) There were differences in scan timing; (4) Whole gland data was not available in all patients due to an inadequate scan trajectory (the scans were

originally performed for tumor analysis); (5) Clinical/physiological data is not available to correlate with the DW-MRI changes; (6) We have used planned dose, rather than the estimated actual delivered dose that would take into account deformation and volume change in the PG and SMG as a result of treatment; (7) DW-MRI is subject to geometric distortion, hampering co-localization of the ROIs on the planning CT and the MRI studies.

Nonetheless, despite these limitations, we have been able to make several observations, including that: salivary gland ADC values rose during and after treatment with both EPI and HASTE DW-MRI techniques and that differences between/within the PG and SMG were observed. In addition, we have observed that different DW-MRI techniques may provide different data.

Conclusions

DW-MRI may merit further investigation as a marker of CRT effect in the salivary glands: the optimum DW-MRI technique and timing needs to be defined, glands should be considered separately and sub-regions within the glands should be analyzed. More detailed understanding of possible heterogeneity in the response to CRT within an individual gland and the relationship between radiotherapy dose and functional effect could help to support the development of sophisticated treatment planning with preferential sparing of specific parts of the salivary glands, in an effort to further reduce the morbidity of CRT [http://clinicaltrials.gov/show/NCT01955239].

References

1. Vissink A, van Luijk P, Langendijk J, Coppes R. Current ideas to reduce or salvage radiation damage to salivary glands. Oral Dis. 2014 Feb 28. doi: 10.1111/odi.12222. [Epub ahead of print]
2. Doornaert P, Verbakel WF, Rietveld DH, Slotman BJ, Senan S. Sparing the contralateral submandibular gland without compromising PTV coverage by using volumetric modulated arc therapy. Radiat Oncol 2011; 6: 74.
3. Nutting CM, Morden JP, Harrington KJ, Urbano TG, Bhide SA, Clark C, et al. PARSPORT trial management group. Parotid-sparing intensity modulated versus conventional radiotherapy in head and neck cancer (PARSPORT): a phase 3 multicentre randomised controlled trial. Lancet Oncol 2011; 12(2): 127-36.
4. Dirix P, De Keyzer F, Vandecaveye V, Stroobants S, Hermans R, Nuyts S. Diffusion-weighted magnetic resonance imaging to evaluate major salivary gland function before and after radiotherapy. Int J Radiat Oncol Biol Phys 2008; 71(5): 1365-71.
5. Verhappen MH, Pouwels PJ, Ljumanovic R, van der Putten L, Knol DL, De Bree R, et al. Diffusion-weighted MR imaging in head and neck cancer: comparison between half-fourier acquired single-shot turbo spin-echo and EPI techniques. AJNR Am J Neuroradiol. 2012 Aug; 33(7): 1239-46.
6. Konings AW, Cotteleer F, Faber H, van Luijk P, Meertens H, Coppes RP. Volume effects and region-dependent radiosensitivity of the parotid gland. Int J Radiat Oncol Biol Phys 2005; 62(4): 1090-5.
7. Coppes RP, Vissink A, Konings AW. Comparison of radiosensitivity of rat parotid and submandibular glands after different radiation schedules. Radiother Oncol 2002; 63(3): 321-8.
8. Teshima K, Murakami R, Yoshida R, Nakayama H, Hiraki A, Hirai T, et al. Histopathological changes in parotid and submandibular glands of patients treated with preoperative chemoradiation therapy for oral cancer. J Radiat Res 2012; 53(3): 492-6.
9. Schouten CS, de Bree R, van der Putten L, Noij DP, Hoekstra OS, Comans EF, et al. Diffusion-weighted EPI- and HASTE-MRI and 18F-FDG-PET-CT early during chemoradiotherapy in advanced head and neck cancer. Quant Imaging Med Surg. 2014 Aug; 4(4): 239-50